Improved Reconstruction of Quantized CT Scans via Genetic Algorithms

Chris Miller, Frank Moore, Brendan Babb
Mathematical Sciences Dept.
University of Alaska Anchorage
Anchorage, AK, USA
affwm@uaa.alaska.edu

Michael R. Peterson
Computer Science Dept.
University of Hawai'i at Hilo
Hilo, HI, USA
mrp@hawaii.edu

***Abstract*—Cost-effective storage and timely transmission of medical images are very difficult technical challenges. Compression and reconstruction techniques must guarantee no significant loss of clinical information. This paper presents a convenient technique for improving the quality of reconstructed computed tomography (CT) images previously subjected to specified levels of lossy compression. Our genetic algorithm (GA) evolves novel transforms that consistently outperform state-of-the-art wavelet-based schemes supported by the Digital Imaging and Communication in Medicine (DICOM) standard.**

Keywords-medical imaging; image reconstruction; wavelets; genetic algorithms; quantization

I. INTRODUCTION

Raw, uncompressed medical images require an enormous volume of storage space [6]. In addition, the time required to electronically transfer medical images over broadband networks is often unacceptable [13]. Lossy compression techniques may be employed to substantially reduce image size. Unfortunately, such techniques also introduce permanent and irreversible information loss in proportion to the amount of compression. Recent studies (e.g., [14]) have established medically acceptable compression ratios of between 8:1 and 15:1 for small images (including computed tomography [CT], ultrasound [US], nuclear medicine [NM], and magnetic resonance imaging [MRI]), and between 20:1 and 30:1 for large images (including computed and digital radiography [CR/DR]).

The JPEG2000 (J2K) digital image compression standard [26] has achieved worldwide acceptance as the state-of-the-art methodology for compressing and reconstructing medical images [9]. The current Digital Imaging and Communication in Medicine (DICOM) standard provides direct support for J2K image compression [23], and this support has the potential to substantially reduce the massive storage and communications requirements of modern Picture Archiving and Communication Systems (PACS). For lossy image compression, J2K utilizes the biorthogonal 9/7 wavelet transform [7]. The 9/7 achieves very high compression ratios without introducing the excessive noise and blocking artifacts of older standards (e.g., JPEG).

Wavelet-based image compression schemes [29] implement the following algorithm:

Step 1: Use a two-dimensional (2D) wavelet transform to decompose a given image **f** into a trend subimage **a** and subimages **h**, **v**, and **d** representing the horizontal, vertical, and diagonal fluctuation. If using multiresolution analysis (MRA) to perform a *k*-level transform, this process will be recursively reapplied to the previous trend subimage.

Step 2: Perform thresholding and quantization to reduce the size of the transformed signal. Thresholding [17] is the process of retaining only the largest transformed values and setting the less significant values to zero; the compressed signal will thus contain significant (non-zero) quantized values, along with a significance map indicating their indices. Quantization [27] is the process representing each signal value using a relatively smaller number of bits (e.g., quantization to an 8-bit signal allows 256 possible values). K:1 uniform scalar quantization maps intervals of width K onto a single quantized value; for example, 64:1 quantization might map values in the range {0, 1, …, 63} to 0, {64, 65, …, 127} to 1, {128, 129, …, 191} to 2, and so on.

Step 3: Transmit the compressed image, which will be much smaller than the original image **f**.

On the receiving end, the compressed image will be dequantized: first, each value is multiplied by the quantization step K, and then half the quantization step will be added to the result. For example, at 64:1 quantization, quantized value 1 might be dequantized to 96, which is the midpoint of the range of values from the original image that might have been quantized to 1. This process of adding half the quantization step back to the dequantized value has the effect of minimizing the average quantization error (assuming that all possible values are equally likely). After dequantization, an inverse 2D wavelet transform will create an approximation of the original image. The difference between the original image and the reconstructed image will primarily be the result of quantization error.

Wavelets [8] are defined using two sets of numbers, known as scaling and wavelet numbers. For the 9/7 inverse (reconstruction) transform, the scaling (*h2*) and wavelet (*g2*) numbers defining the low-pass and high-pass synthesis filters (rounded to four decimal places) are

$h2$ = [-0.0645, -0.0407, 0.4181, 0.7885, 0.4181, -0.0407, -0.0645]

$g2$ = [0.0378, 0.0239, -0.1106, -0.3774, 0.8527, -0.3774, -0.1106, 0.0239, 0.0378]

Since 2004, several researchers have used various forms of evolutionary computation (EC), including genetic algorithms (GAs) [10], to evolve sets of wavelet and scaling numbers describing new transforms capable of reducing the mean squared error (MSE) observed in reconstructed signals subjected to quantization error, while continuing to match or exceed the compression capabilities of standard wavelet transforms. Grasemann and Mikkulainen ([11], [12]) combined a GA with the lifting scheme [25] to synthesize new wavelet transforms from an existing wavelet filter; the new wavelets exhibited improved performance for specific classes of images. Moore [21] used a GA to optimize image reconstruction transforms; his technique differed from that of Grasemann and Mikkulainen, however, in that it did not impose specific mathematical properties required of wavelets (such as conservation of energy) upon the evolved solutions. The resulting transforms exhibited modest improvements over wavelet reconstruction transforms at various quantization levels. Babb, Becke, and Moore [2] expanded upon this technique by simultaneously evolving matched compression and reconstruction transform pairs, and added the capability of evolving multiresolution analysis (MRA) transforms [20]. Their approach seeded the initial population with one exact copy and many randomly mutated copies of a selected wavelet; thus, each of the transforms in the evolving population had the same structure as the wavelet, but contained wavelet and scaling numbers optimized by the GA. For MRA transforms [17], these researchers found it advantageous to evolve different coefficients at every multiresolution level; evolving a four-level matched compression and reconstruction transform having the same structure as the 9/7, for example, requires simultaneous optimization of 128 floating-point numbers, resulting in a considerably large and complex search space.

To date, researchers have successfully optimized transforms that outperform wavelets in each of the following lossy image compression domains for which wavelets were previously considered state-of-the-art:

(a) Digital photographs, such as the classic “Lenna”, “Goldhill”, “Airplane”, and “Baboon” [21].
(b) Fingerprints from the US Federal Bureau of Investigation (FBI) database [3].
(c) Satellite images such as “Downtown Baghdad”, “Air Force Museum”, and “Pearl Harbor” ([5], [4]).
(d) Images of the planet Mars transmitted from rovers “Spirit” and “Opportunity” [1].
(e) US images [18]. This study appears to have been the first time that an EC-based approach has been used to evolve optimized image reconstruction transforms specifically for a medical imaging application. The results of this study were very encouraging, with MSE reductions as high as 53.44% (3.32 dB) in comparison to the 9/7 at 64:1 quantization.

II. CT Images

The data storage needs of medical facilities are growing at an annual rate exceeding 50%, with most of that need being driven by image storage [28]. In 2010, approximately 72 million computed tomography (CT) scans were performed in the United States [19]. Assuming 16-bit resolution, the size of a single 512-by-512-pixel computed tomography (CT) image slice is about 0.5 megabyte (MB); a typical CT image consists of about 200 slices, making the average total size of a single CT scan about 100 MB [30]. Retrieval of a CT scan, even at the same hospital, may take as long as 15 minutes [16]. In addition, widespread use of teleradiology and telemedicine necessitate the availability of high-speed, secure medical image transmission technology [24].

III. Experiments and results

The primary question addressed by this research is:

Can EC be used to optimize compression transforms that outperform the 9/7 wavelet for the lossy compression of CT scans?

To begin answering this question, we conducted a series of experiments using a GA characterized as follows:

(a) Population size M = 200.
(b) Maximum number of generations G = 5000, with early termination after 250 generations with no improvement over the current best-of-run individual.
(c) Crossover percentage p_c = 80%.
(d) Mutation percentage p_m = 20% per individual. For each individual selected for mutation, each wavelet and scaling number had a 10% likelihood of undergoing mutation. Mutation was Gaussian with Standard deviation = 0.3 and shrink rate = 1.
(e) Elitism = 1 (i.e., the best individual from each generation was copied, unchanged, into the next generation, thus guaranteeing no decrease in the best individual’s fitness from one generation to the next).
(f) Each candidate solution consisted of 16 floating-point values. The initial population for each run (generation 0) was seeded with one exact copy and M-1 randomly mutated copies of the scaling and wavelet numbers from the 9/7 wavelet’s reconstruction transform.

Note that these settings are identical to those used to evolve optimized transforms for US image reconstruction [18].

We conducted three sets of training runs using a quantization step of 16:1, 32:1, and 64:1, respectively. Each training run used a unique combination of training image (a single randomly selected CT image slice) and random number seed. Each run ran to quiescence, producing a unique best-of-run transform. Each best-of-run transform was subsequently tested on the remaining image slices from the test set (a technique similar to “leave-1-out” cross validation [15]). The specific CT scan used in this research consisted of a set of 30 noncontrast axial brain images taken at Alaska Regional Hospital for diagnosis of a potentially severe medical emergency.

Fig. 1 lists the training image used, the amount of quantization used during training, and the best-of-run individual's average MSE reduction (in comparison to the 9/7 wavelet) when subsequently tested against the remaining 29 images from the test set at under conditions subject to 16:1, 32:1, and 64:1 quantization. Fig. 2 shows a typical image from the test set (m4.bmp). Fig. 3 illustrates the same image after compression by the 9/7 forward transform, 32:1 quantization, dequantization, and reconstruction by the 9/7 inverse transform. Fig. 4 shows the image after reconstruction by an evolved transform.

For this image, the best evolved transform (from run 18) reduced MSE by 12.65% (0.59 dB) in comparison to the 9/7's reconstructed image. Unfortunately, differences of this magnitude are difficult to discern with the naked eye. To more effectively visualize the superiority of the evolved transform, we developed MATLAB scripts to create error images according to the following algorithm:

1. Calculate raw error as the difference between the two images.
2. Multiply raw error by 4 to emphasize it.
3. Add 128 to all values, shifting from range -128…127 to range 0…255.
4. Apply a custom color map that is symmetric around 128. Pixels with zero error will equal 128. The further away a pixel is from this value, the greater its error. Errors increase from white to yellow to red to black.

	Training	Training	Testing Quantization		
Run	**Image**	**Quantization**	**Q = 16:1**	**Q = 32:1**	**Q = 64:1**
1	m4	16:1	-5.42%	3.90%	-6.49%
2	m4	16:1	-3.36%	4.22%	-3.01%
3	m4	16:1	-3.46%	4.22%	0.47%
4	m7	16:1	4.39%	4.21%	-3.16%
5	m7	16:1	4.36%	3.88%	-9.12%
6	m7	16:1	4.28%	3.86%	-9.11%
7	m11	16:1	-75.09%	-13.20%	5.48%
8	m11	16:1	-64.84%	-8.12%	5.73%
9	m11	16:1	-86.71%	-15.92%	5.63%
10	m4	32:1	-27.03%	1.43%	-10.45%
11	m4	32:1	-23.40%	3.16%	-10.41%
12	m4	32:1	-25.39%	2.31%	-10.29%
13	m5	32:1	-24.41%	3.12%	-10.24%
14	m5	32:1	-20.79%	4.27%	-10.06%
15	m5	32:1	-22.99%	4.21%	-9.15%
16	m7	32:1	-16.51%	5.25%	1.45%
17	m7	32:1	-17.71%	5.03%	-3.77%
18	m7	32:1	-18.78%	5.13%	-2.75%
19	m11	32:1	2.86%	5.56%	3.75%
20	m11	32:1	2.57%	5.95%	3.80%
21	m11	32:1	-0.50%	5.74%	4.01%
22	m17	32:1	-7.14%	4.92%	4.05%
23	m17	32:1	-17.68%	4.36%	4.16%
24	m17	32:1	-19.84%	4.10%	4.27%
25	m11	64:1	-82.67%	-17.72%	5.44%
26	m11	64:1	-67.56%	-9.67%	5.67%
27	m11	64:1	-79.78%	-11.86%	5.72%
28	m15	64:1	-110.99%	-26.57%	2.00%
29	m15	64:1	-120.78%	-33.22%	1.56%
30	m15	64:1	-126.68%	-36.88%	1.67%
31	m17	64:1	-107.77%	-27.17%	1.64%
32	m17	64:1	-103.74%	-23.73%	1.92%
33	m17	64:1	-106.04%	-24.65%	4.75%

Figure 1. Test results for transforms evolved using specific training images and under conditions subject to specific quantization levels.

Figure 2. A typical CT image.

Figure 3. The image after reconstruction by the 9/7 wavelet.

Figure 4. The image reconstructed by an evolved transform. Differences of this magnitude are difficult to discern with the naked eye.

The first error image (Fig. 5) shows the difference between the original CT image (Fig. 2) and the wavelet-reconstructed image (Fig. 3), while the second error image (Fig. 6) shows that difference for the image reconstructed by the evolved transform (Fig. 4). The generally lighter color of Fig. 6 (in comparison to Fig. 5) highlights the degree to which the evolved transform outperforms the wavelet for the reconstruction of CT images subjected to lossy compression.

Fig. 7 visualizes the difference in MSE between the images produced by the wavelet and evolved filter on a pixel-by-pixel basis. This image was created from the wavelet error matrix and the evolved transform error matrix (rather than from the

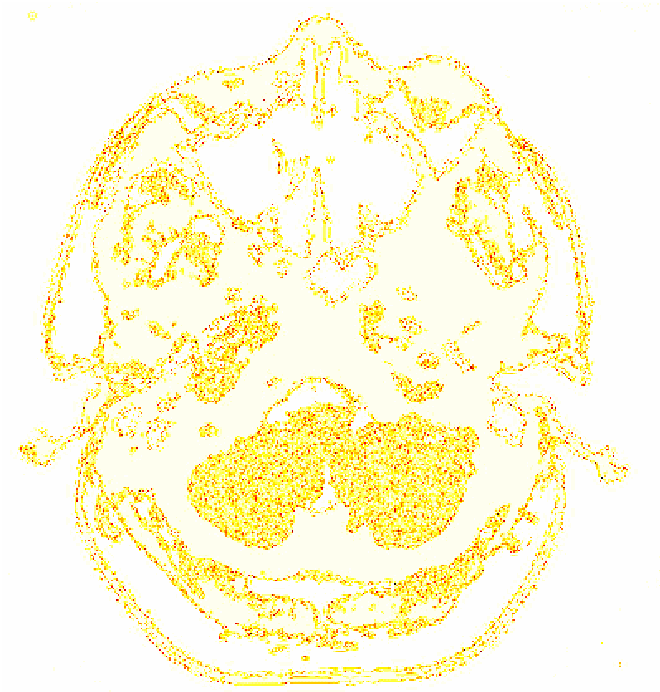

Figure 5. The difference image for the 9/7 wavelet. Darker points indicate greater error.

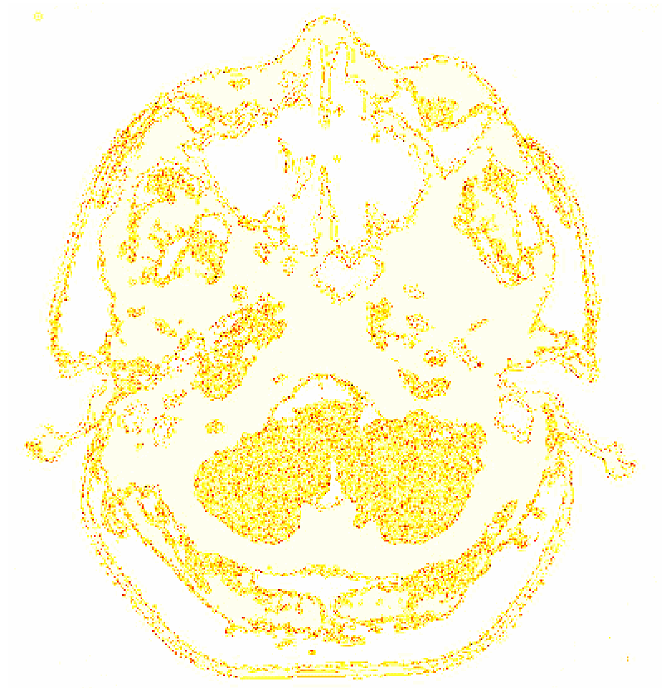

Figure 6. The evolved transform's difference image. Generally lighter color indicates less error than was introduced by the 9/7.

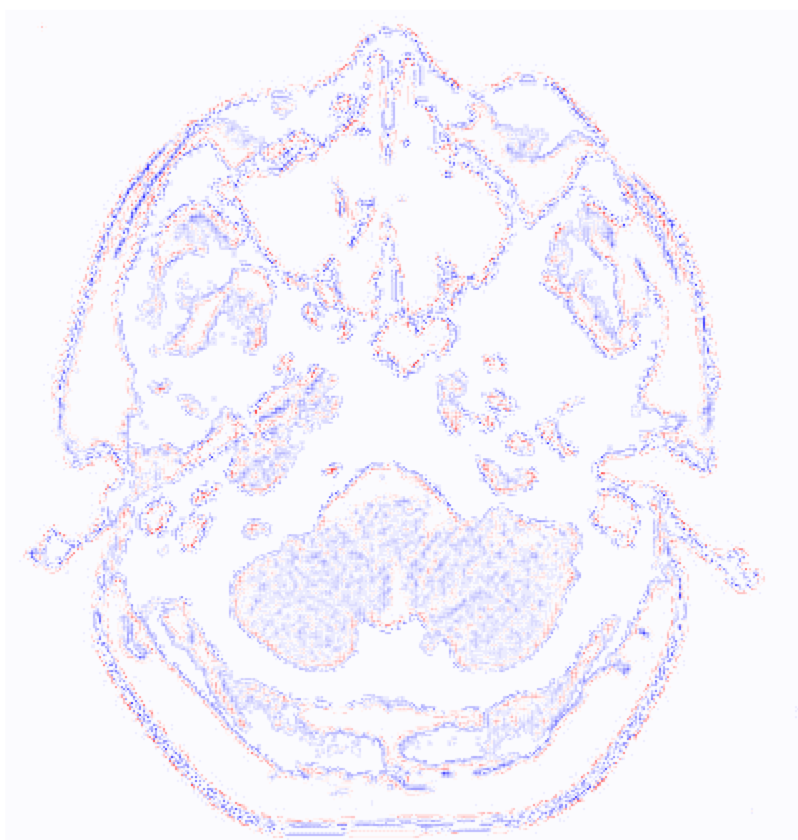

Figure 7. A pixel-by-pixel visualization of the difference in errors created by the wavelet and evolved reconstruction transform. The blue pixels indicate where the 9/7 introduced greater error, while the red pixels indicate where the evolved transform's error was greater.

reconstructed images) using the algorithm described above. Blue indicates pixels for which the 9/7 accumulated more error, while red indicates pixels where the evolved transform produced greater error. The darker the pixel, the bigger the difference. The larger number and darker color of blue pixels in Fig. 7 demonstrate the overall superiority of the evolved transform.

These results appear to support the following conclusions:

(a) It is possible to evolve a reconstruction transform that outperforms the 9/7 wavelet transform for the reconstruction of CT images under conditions subject to a specified amount of quantization.

(b) In all but one run (run 24), the performance of transforms optimized at 32:1 or 64:1 quantization degrades – often substantially – when subsequently tested at different quantization levels. In contrast, the performance of transforms optimized at 16:1 quantization was quite unpredictable, and often improved when tested at higher quantization levels. Further research will be necessary to explain these results.

(c) In only two runs (runs 19 and 20) were transforms evolved that outperformed the 9/7 wavelet at all three quantization levels. These results remind us of the complexity of searching for optimized solutions in a nonlinear, 16-dimensional floating-point space.

(d) GAs are stochastic processes. Several runs are typically necessary to produce an individual whose performance generalizes well during subsequent testing against images not specifically included in the training population; many runs will fail to produce such an individual. Here, the best-of-run individuals evolved for 12 of our 45 runs were overtrained on the training image and failed to outperform the 9/7 wavelet at ANY quantization level when subsequently tested against the remaining 29 images from the test set.

(e) MSE reductions for CT scans observed during this research effort were much smaller than we previously observed for US images. Whereas average MSE reductions of 15.84% (0.75 dB), 49.81% (2.99 dB), and 53.44% (3.32 dB) were observed on the US image test set at 16:1, 32:1, and 64:1 quantization, respectively [18], the best average MSE reductions for the CT image test at corresponding quantization levels were only 4.39% (0.195 dB), 5.95% (0.266 dB), and 5.72% (0.256 dB). This result may be due to the fact that US images tend to be quite "fuzzy" even before being subjected to lossy compression, whereas the images from a CT scan are much "sharper" and may be subjected to higher quantization levels before substantial amounts of error are introduced.

IV. Conclusions

The research summarized by this paper demonstrates that it is possible to use a GA to evolve wavelet and scaling numbers for transforms that outperform the 9/7 wavelet for the reconstruction of images from CT scans under conditions subject to quantization error. Simply put, evolved transforms provide better image quality at identical levels of compression. These results thus establish a new state-of-the-art for reconstructing CT scans.

The next step in this research will be to determine the maximum amount of compression of CT scans that can be achieved by an evolved transform capable of matching the medically acceptable amount of noise achieved by the current 9/7 wavelet-based standard [14]. To complete this step, many more runs with larger values for M and G will be required. A positive result would reduce the amount of storage and transmission bandwidth required for compressed CT scans without adversely affecting the overall clinical quality of those images. In addition, the use of multiple training images in future research should reduce the likelihood of overtraining.

The predominance of blue pixels in Fig. 7 indicates that the evolved transform generally outperformed the wavelet. Nevertheless, Fig. 7 contains many red pixels indicating areas within the image for which the wavelet produced less error. These red areas tend to congregate along the sharpest edges of the image. Previous studies [22] have demonstrated the utility of using an edge detection method of evolving two filters (one for reconstruction near edges and one for reconstructing the remainder of the image). Future research should incorporate this technique to further enhance the performance of evolved transforms.

The methodology established by the previous study [18] and continued during this research will be applied to other types of medical images (NM, MRI, CR, and DR). We anticipate similarly impressive results which, if achieved, could have a substantial impact upon state-of-the-art medical image compression technology.

References

[1] S. Aldridge, B. Babb, F. Moore, and M. R. Peterson, "Improved lossy compression of deep space images via genetic algorithms," 2010, in press.

[2] B. Babb, S. Becke, and F. Moore, "Evolving optimized matched forward and inverse transform pairs via genetic algorithms," Proceedings of the 48th IEEE International Midwest Symp. Circuits and Systems: Cincinnati, OH, 8/7-10, 2005.

[3] B. Babb and F. Moore, "The best fingerprint compression standard yet," Proceedings of the 2007 IEEE International Conf. Systems, Man, and Cybernetics, 10/7-10, 2007, Montreal, Quebec, Canada, IEEE.

[4] B. Babb, F. Moore, and M. R. Peterson, "Improved multiresolution analysis transforms for satellite image compression and reconstruction using evolution strategies," Proc. Eleventh Annual Genetic and Evolutionary Computation Conf., Montreal, QC, Canada, 7/8-12, 2009.

[5] B. Babb, F. Moore, M. R. Peterson, and G. Lamont, "Improved satellite image compression and reconstruction via genetic algorithms," Electro-Optical Remote Sensing, Photonic Technologies, and Applications II, SPIE Symp. Optics/Photonics in Security & Defence, Cardiff, UK, 9/15-18, 2008.

[6] M. Choong, R. Logeswaran, and R. Bister, "Cost-effective handling of digital medical images in the telemedicine environment," International J. Medical Informatics, vol. 76 (9), pp. 646-654, 2007.

[7] A. Cohen, I. Daubechies, and J. Feauveau, "Biorthogonal bases of compactly supported wavelets," Comm. Pure and Applied Mathematics, vol. 45, pp. 485-560, 1992.

[8] I. Daubechies, Ten Lectures on Wavelets, SIAM, 1992.

[9] D. Foos, E. Muka, R. Slone, B. Erickson, M. Flynn, D. Clunie, L. Hildebrand, K. Kohm, and S. Young, “JPEG 2000 compression of medical imagery,” SPIE Vol. 3980: PACS Design and Evaluation: Engineering and Clinical Issues, 2000.

[10] D. Goldberg, Genetic Algorithms in Search, Optimization, and Machine Learning, Addison-Wesley, 1989.

[11] U. Grasemann and R. Mikkulainen, “Evolving wavelets using a coevolutionary genetic algorithm and lifting,” Proc. Sixth Genetic and Evolutionary Computation Conf., vol. II, pp. 969-980, 2004.

[12] U. Grasemann and R. Mikkulainen, “Effective image compression using evolved wavelets,” Proc. Seventh Annual Genetic and Evolutionary Computation Conf., 6/25-29, 2005, Washington, DC, USA, vol. 2, pp. 1961-1968.

[13] H. Huang, “Enterprise PACS and image distribution,” Computerized Medical Imaging and Graphics, vol. 27 (2, 3), pp. 241-253, 2003.

[14] D. Koff, “Invited review: Canadian PACS – cost effective and safe – the adoption of image compression for diagnostic purposes,” Proc. UK Radiological Congress 2008, British Institute of Radiology.

[15] P. Lachenbruch and M. Mickey, “Estimation of error rates in discriminant analysis,” Technometrics, vol. 10 (1), pp. 1-11, 1968.

[16] M. Leiserson, “The future of medical imaging,” TuftScope: The Interdisciplinary J. of Health, Ethics, and Policy, vol. 9 (II), pp. 17-18, 2010.

[17] S. Mallat, A Wavelet Tour of Signal Processing (2nd Ed.), Academic Press, 1999.

[18] C. Miller, B. Babb, F. Moore, and M. R. Peterson, “Evolving improved transforms for reconstruction of quantized ultrasound images,” Proc. IEEE Workshop on Applications of Computer Vision, Kona, HI, USA, January 5-7, 2011.

[19] J. Miller, “CT and radiation issues,” Radiology Rounds, vol. 8 (3), March 2010.

[20] F. Moore, “A genetic algorithm for evolving improved MRA transforms,” WSEAS Trans. Signal Proc., vol. 1 (1), pp. 97-104, 2005.

[21] F. Moore, P. Marshall, and E. Balster, “Evolved transforms for image reconstruction,” Proc. IEEE Congress on Evolutionary Computation (CEC 2005), Edinburgh, Scotland, UK, 9/02-05, 2005.

[22] M. R. Peterson and G. Lamont, “Improving image resolution with edge-targeted filter evolution,” Proc. IEEE Aerospace Conf., Big Sky, MT, 3/1-8, 2008, pp. 1-14.

[23] O. Pianykh, Digital Imaging and Communications in Medicine (DICOM) -- A Practical Introduction and Survival Guide, Springer, 2008.

[24] P. Puech, E. Chazard, L. Lemaitre, and R. Beuscart, “DicomWorks teleradiology: secure transmission of medical images over the internet at low cost,” Proc. 29th Annual International Conf. IEEE Engineering in Medicine and Biology Society (EMBS), Lyon, France, 8/23-26, 2007.

[25] W. Sweldens, “The lifting scheme: a custom-design construction of biorthogonal wavelets,” Applied and Computational Harmonic Analysis, vol. 3, pp. 186-200, 1996.

[26] D. Taubman and M. Marcellin, JPEG2000: Image Compression Fundamentals, Standards, and Practice, Kluwer Academic Publishers, 2002.

[27] M. Vetterli and J. Kovacevic, Wavelets and Subband Coding, Prentice Hall, 1995.

[28] B. Walker, “Everything in its place: storing large medical images and records,” Rt-image, 1/19/2009.

[29] J. Walker, A Primer on Wavelets and their Scientific Applications (2nd Ed.), Chapman & Hall/CRC Press, 2008.

[30] Y. Wu, “From CT image to 3D model,” Advanced Imaging, pp. 20-23, August 2001.